INFECTION AND IMMUNITY, Jan. 2008, p. 278–288 Vol. 76, No. 1
0019-9567/08/$08.00+0 doi:10.1128/IAI.00636-07

Autophagy during Proliferation and Encystation in the Protozoan Parasite *Entamoeba invadens*[▽]

Karina Picazarri, Kumiko Nakada-Tsukui, and Tomoyoshi Nozaki*

Department of Parasitology, Gunma University Graduate School of Medicine, Maebashi, Gunma 371-8511, Japan

Received 7 May 2007/Returned for modification 13 June 2007/Accepted 29 September 2007

Autophagy is one of the three systems responsible for the degradation of cytosolic proteins and organelles. Autophagy has been implicated in the stress response to starvation, antigen cross-presentation, the defense against invading bacteria and viruses, differentiation, and development. *Saccharomyces cerevisiae* Atg8 and its mammalian ortholog, LC3, play an essential role in autophagy. The intestinal protozoan parasite *Entamoeba histolytica* and a related reptilian species, *Entamoeba invadens*, possess the Atg8 conjugation system, consisting of Atg8, Atg4, Atg3, and Atg7, but lack the Atg5-to-Atg12 conjugation system. Immunofluorescence imaging revealed that polymorphic Atg8-associated structures emerged in the logarithmic growth phase and decreased in the stationary phase and also increased in the early phase of encystation in *E. invadens*. Immunoblot analysis showed that the increase in phosphatidylethanolamine-conjugated membrane-associated Atg8 was also accompanied by the emergence of Atg8-associated structures during the proliferation and differentiation mentioned above. Specific inhibitors of class I and III phosphatidylinositol 3-kinases simultaneously inhibited both the growth of trophozoites and autophagy and also both encystation and autophagy in *E. invadens*. These results suggest that the core machinery for autophagy is conserved and plays an important role during proliferation and differentiation in *Entamoeba*.

Amoebiasis is a diarrheal disease caused by the protozoan parasite *Entamoeba histolytica* and affects approximately 50 million inhabitants of areas where the disease is endemic, resulting in an estimated 40,000 to 110,000 deaths annually (61). Its transmission occurs through the ingestion of food or water contaminated with infective cysts (33). Although encystation is an essential fundamental process required for the transmission of the disease, little is known about biochemical and cell biological changes or the regulation of gene expression that occurs during this process except in some cases (5, 7, 10–12, 47, 57). In the reptilian *Entamoeba* species *E. invadens*, 18 genes, including those for ubiquitin 48, gene 122 (47), chitinases 1 and 2 (7, 57), two isoforms of chitin synthases (chs-1 and chs-2) (5), and the cyst-specific lectins called Jacob (7) and Jessie (5, 57), were differentially expressed at different stages of encystation. However, various fundamental events that occur during encystation, which allow drastic changes in cellular compositions and organelle structures, remain largely uncharacterized except for the involvement of proteasomes (12). Recently, a transcriptome of *E. histolytica* clinical isolates which identified some novel *E. invadens* stage-specific genes has been documented (10).

Autophagy is a cellular process highly conserved in eukaryotes which permits the degradation of long-lived proteins and damaged or unnecessary organelles (24). Autophagy has been implicated in various biological processes, including the stress response to carbon and nitrogen starvation; antigen cross-presentation; the defense against invading bacteria, viruses, and other intracellular pathogens; differentiation; and development (15, 25, 28, 30, 38, 49, 51). Autophagosome formation is initiated by the emergence of an isolation membrane in the cytosol, called the preautophagosomal structure (PAS) (36, 50, 58). The PAS elongates and expands to form the autophagosome membranes (19, 25, 36) that enclose cytosolic components and organelles, including mitochondria and endosomes (14, 18, 45). Autophagosomes subsequently fuse to lysosomes, leading to the degradation of sequestered organelles and materials (15, 25). In *Saccharomyces cerevisiae*, 16 autophagy-related (*Atg*) genes that encode components essential for autophagy were identified (21). Autophagosome formation is regulated by two related ubiquitin-like (UBL) systems in both yeast and mammals (25, 54). The first UBL system allows the conjugation of Atg12 to Atg5. After the Atg12-to-Atg5 conjugation, these proteins form a complex with Atg16 (22), and this complex acts upstream of the second conjugation system. In the second conjugation system, where Atg8 is a major anchoring molecule, Atg4 protease (54) exposes the terminal glycine of Atg8 (36). Atg8 is subsequently activated by the E1 enzyme Atg7 (54) and transferred to Atg3, an E2-like enzyme, which conjugates Atg8 to phosphatidylethanolamine (PE) (17). Atg4 also participates in Atg8 deconjugation, which is essential for the fusion of autophagosomes with lysosomes/vacuoles (2, 4, 20, 54, 62). Among the components involved in these conjugation systems, Atg8 has been considered to be an authentic marker for autophagosomes because lipid-anchored Atg8 remains attached to the inner membrane of autophagosomes until it is degraded by lysosomal hydrolases after the fusion with lysosomes (36).

The biological importance of autophagy has been demonstrated both in vitro and in vivo with various organisms (9, 16, 23, 29, 44, 63). In *Caenorhabditis elegans*, the inhibition of *Atg1*, *Atg6*, *Atg7*, *Atg8*, and *Atg10* by RNA interference resulted in a defect in the organism's morphogenesis to the dauer stage,

* Corresponding author. Mailing address: Department of Parasitology, Gunma University Graduate School of Medicine, 3-39-22 Showa-machi, Maebashi, Gunma 371-8511, Japan. Phone: 81 27 220 8020. Fax: 81 27 220 8025. E-mail: nozaki@med.gunma-u.ac.jp.
▽ Published ahead of print on 8 October 2007.

when the organism takes a dormant form between the L2 and L3 larval stages under conditions of high population density, reduced levels of nutrients, or increased temperature. Under such conditions, development ceases so that the organism can survive for an extended period (34). In the social ameba *Dictyostelium discoideum*, Atg8 plays a role in survival and spore formation. During starvation, *D. discoideum* develops a multicellular form that functions like a spore reservoir. A mutant lacking *Atg5* or *Atg7* was unable to produce viable, mature spores, and autophagosome formation was abolished under conditions of starvation (41). A *Leishmania major vps4* mutant which showed a defect in endosomal sorting and the fusion of Atg8 autophagosomes with lysosomes failed to differentiate from a diving procyclic promastigote into the infective metacyclic form (4).

In this study, we show by a genome-wide survey that *E. histolytica* and the related reptilian species *Entamoeba dispar* and *E. invadens* possess genes involved in the Atg8 conjugation but not those of the Atg5-to-Atg12 conjugation pathway. Furthermore, we demonstrate, by immunoblot and immunofluorescence assays, that autophagy occurs in two independent phases—the logarithmic growth phase and the early phase of encystation—in the life cycle of *E. invadens*.

MATERIALS AND METHODS

Bacteria, chemicals, and reagents. The *Escherichia coli* DH5α and BL21(DE3) strains were purchased from Life Technologies (Tokyo, Japan) and Invitrogen (Tokyo, Japan), respectively. All chemicals were of analytical grade and were purchased from Sigma-Aldrich (Tokyo, Japan) or Wako (Tokyo, Japan) unless otherwise stated.

***E. invadens* culture and encystation.** Trophozoites of the *E. invadens* IP-1 strain were cultured axenically in BI-S-33 medium at 26°C. To induce encystation, 2-week-old *E. invadens* cultures were passaged in 47% LG medium lacking glucose (47) at approximately 6×10^5 cells/ml. Amoebae were collected at various time points, and the formation of cysts was assessed by virtue of the resistance to 0.05% Sarkosyl using 0.22% trypan blue to selectively stain dead cells. Cysts were also verified by cyst wall staining by incubating amoebae with calcofluor white (fluorescent brightener 28; Sigma-Aldrich) at room temperature.

Genome-wide survey of genes involved in autophagy in *Entamoeba*. *S. cerevisiae* Atg proteins were obtained from the NCBI nonredundant protein database (http://www.ncbi.nlm.nih.gov/) and used as queries to search for orthologs in the *E. histolytica*, *E. dispar*, and *E. invadens* genome databases (http://www.tigr.org/tdb/e2k1/eha1, http://www.sanger.ac.uk/Projects/E_histolytica/, http://www.sanger.ac.uk/Projects/E_dispar/, and http://www.sanger.ac.uk/Projects/E_invadens). Possible orthologs were further analyzed with the blastp algorithm (http://www.ncbi.nlm.nih.gov/BLAST/) against the nonredundant database at NCBI to find the closest homologs in other organisms.

Production of recombinant Eh*Atg8* and antiserum against EhAtg8. Standard techniques were used for routine DNA manipulation, subcloning, and plasmid construction as previously described (46). The protein coding region of *E. histolytica Atg8a* (Eh*Atg8a*) (locus tag XP_649165) was amplified using oligonucleotide primers (5′-CATCCCGGGATGGAATCACAACCAAAACTT-3′ and 5′-AGACTCGAGTTAATTTCCAAAGACAGATTC-3′) and the *E. histolytica* cDNA library (39) by PCR. The parameters used for the PCR were an initial step of denaturation at 94°C for 2 min, followed by 30 cycles of denaturation at 94°C for 15 s, annealing at 55°C for 30 s, and an extension at 65°C for 1 min. A final step of denaturation at 95°C for 9 s, annealing at 60°C for 9 s, and an extension at 95°C for 9 s was used to remove primer dimers. A 408-bp PCR fragment was cloned in the SmaI-XhoI site of the pGEX-6P-2 expression vector (GE Healthcare Bioscience, Tokyo, Japan) to produce pGST-EhAtg8. The pGST-EhAtg8 plasmid was introduced into the *E. coli* BL21(DE3) strain. The expression of the glutathione *S*-transferase (GST)-EhAtg8 recombinant protein was induced, and cell lysate was produced according to the instructions of the manufacturer. The GST tag at the amino terminus of the recombinant GST-EhAtg8 construct was cleaved by Precision protease (GE Healthcare Bioscience) and removed by GSTrap (GE Healthcare Bioscience). The recombinant EhAtg8 protein was further purified by Mono Q anion-exchange chromatography on an AKTA Explorer chromatograph (GE Healthcare Bioscience). Rabbit antiserum against EhAtg8 was commercially produced (Kitayama Rabesu, Nagano, Japan).

Cell fractionation. Amoebae were harvested, washed with phosphate-buffered saline containing 2% glucose, and resuspended in a homogenization buffer (50 mM Tris, pH 7.5; 250 mM sucrose; 50 mM NaCl; and 1.34 mM *trans*-epoxysuccinyl-L-leucylamido-[4-guanidino butane]). The amoebae were homogenized with 80 to 300 strokes (depending on the percentage of cysts) in a glass homogenizer and centrifuged at $400 \times g$ for 5 min at 4°C to remove unbroken cells. The supernatant was further centrifuged at $100,000 \times g$ for 1 h to separate a high-speed pellet from the supernatant, both of which were subjected to immunoblot analysis.

Immunoblot analysis. To differentiate unmodified and PE-conjugated Atg8, sodium dodecyl sulfate-polyacrylamide gel electrophoresis (SDS-PAGE) was conducted using 13.5% separating gel containing 6 M urea, as previously described (20). Approximately 5 μg of lysates or fractions were separated by denaturing SDS-PAGE and transferred to nitrocellulose membranes. After the membranes were blocked with 5% skim milk, they were incubated with anti-EhAtg8 or anti-EhNifS (1) antibody (1/1,000 dilution) for 1 h. After being washed, the membranes were incubated with anti-rabbit immunoglobulin G (IgG) alkaline phosphatase-conjugated antibody (Jackson Laboratories, Bar Harbor, ME) or horseradish peroxidase-conjugated antibody (Amersham Bioscience, Piscataway, NJ) for 1 h. Proteins were visualized with an alkaline phosphatase conjugate substrate kit (Bio-Rad, Hercules, CA) or by chemiluminescence with the Immobilon Western substrate (Millipore Corporation, Billerica, MA). The intensity of the bands visualized by chemiluminescence was detected on a Lumi-Imager F1 workstation (Roche Applied Science, Tokyo, Japan) with the LumiAnalyst software (Roche Applied Science) and further analyzed with ImageJ.

Indirect immunofluorescence assay. Trophozoites and cysts were fixed in 3.7% paraformaldehyde in phosphate-buffered saline for 10 min at room temperature, washed, and permeabilized with 0.2% saponin for 10 min. Then, the cells were incubated with anti-EhAtg8 antibody (1/1,000 dilution) for 1 h at room temperature and subsequently incubated with anti-rabbit IgG Alexa Flour 488 antibody (Invitrogen) for 1 h at room temperature. Finally, the cells were washed, mounted on a glass slide, and examined under a confocal laser scanning microscope (LSM 510 Meta; Carl Zeiss, Thornwood, NY). The images were further analyzed with LSM 510 software.

Nucleotide and protein sequence accession numbers. The nucleotide and protein sequences reported in this paper have been submitted to the DDBJ with accession numbers AB326955 (*E. invadens Atg8* [Ei*Atg8*]) and AB326956 (Ei*Atg3*).

RESULTS AND DISCUSSION

One of the two UBL systems is conserved in *E. histolytica*. In yeast and mammals, the biogenesis of autophagosomes is regulated by two UBL systems (25, 54). The *E. histolytica* genome (HM-1:IMSS [8]) apparently encodes only one of the two UBL systems (Table 1). We identified genes encoding two Atg8 proteins (designated EhAtg8a and EhAtg8b), four Atg4 proteins (designated EhAtg4a to EhAtg4d), one Atg7 protein, and one Atg3 protein. The two EhAtg8 proteins showed 96% identity to each other. EhAtg8a and EhAtg8b showed 31 to 33, 25 to 27, and 28 to 30% identity to bee *Apis mellifera* Atg8a, yeast Atg8, and γ-aminobutyric acid receptor-like 2 (Gabarapl2) from amphioxus *Branchiostoma belcheri tsingtauense*, respectively, the last of which was shown to be expressed during the early embryo and larval development phases (26).

EhAtg4a to EhAtg4d showed 22 to 26% identity to yeast and mammalian Atg4. Atg4 belongs to a new class of cysteine proteases (CPs) (20), which differ in function and structure from other CPs, such as the papain, HAUSP, UCH-L3, and Ulp1 families (52). EhAtg4s lack a prodomain typically present in most amoebic CPs. In addition, the active-site cysteines that are well conserved among cathepsin L-like CPs, e.g., CP1, CP2, and CP5, are not aligned with those in these Atg4s (data not

TABLE 1. The Atg8 conjugation system is conserved in *E. histolytica*

S. cerevisiae protein name	Accession no.[a]	Putative EhAtg	*E. histolytica* locus tag/accession no.[b]	E value against *S. cerevisiae* ortholog	Best hit: Organism, locus tag or accession no. (protein name)[a]	Best hit: E value	Best hit against mammals: Organism, locus tag or accession no. (protein name)[a]	Best hit against mammals: E value
Atg8	P38182	Atg8a	XP_649165/337.m00048	4e−6	*A. mellifera*, XP_001120069 (Atg8a)	7e−8	*Pan troglodytes*, XP_511114 (Gabarapl2)	5e−7
		Atg8b	XP_649940/258.m00050	2e−4	*A. mellifera*, XP_001120069 (Atg8a)	4e−7	*Macaca mulatta*, XP_001104154 (Gabarapl2)	1e−6
Atg4	P53867	Atg4a	XP_653798/72.m00167	6e−12	*Strongylocentrotus purpuratus*, XP_786847 (autophagy-related 4D)	7e−17	*Canis familiaris*, XP_851977 (CP Apg4b)	2e−13
		Atg4b	XP_656724/8.m00420	5e−12	*Trypanosoma brucei*, XP_829686 (peptidase)	1e−14	*Pan troglodytes*, XP_001145426 (CP Atg4a)	4e−11
		Atg4c	XP_652043/134.m00147	5e−8	*Trypanosoma cruzi*, XP_813094 (Atg4)	4e−6	*Bos taurus*, XP_873804 (cysteine endopeptidase AUTLlike 4)	1e−5
		Atg4d	XP_651386/168.m00116	6e−6	*Bos taurus*, Q6PZ05 (CP Atg4a)	1e−11	*Bos taurus*, Q6PZ05 (CP Atg4a)	4e−11
Atg7	P38862	Atg7	XP_654007/65.m00164	1e−104	*D. discoideum*, XP_645809 (autophagy protein 7)	6e−108	*M. musculus*, NP_083111 (autophagy-related protein 7)	2e−102
Atg3	P40344	Atg3	XP_654705/46.m00258	5e−29	*Strongylocentrotus purpuratus*, XP_001175772 (similar to MGC80121 protein)	3e−37	*Rattus norvegicus*, Q6AZ50 (autophagy-related protein 3)	2e−26
Atg5	Q12380		XP_651022/186.m00113	6.3e−1	*Anopheles gambiae*, BAC82595 (reverse transcriptase)	1e−8	*Canis familiaris*, XP_851237 (LINE-1 reverse transcriptase)	7e−2
Atg10	Q07879		XP_650961/190.m00098	4.5e−1	*Gibberella zeae*, XP_390739 (hypothetical protein)	1.7	*Canis familiaris*, XP_534421 (similar to chromodomain helicase DNA binding protein 6)	2.8
Atg12	P38316		XP_650304/229.m00072	6e−2	*Ostreococcus tauri*, CAL57467 (kinesin, putative)	2e−3	*Canis familiaris*, XP_848707 (similar to myosin, heavy polypeptide 7, cardiac muscle)	4e−3
Atg16	Q03818		XP_654748/45.m00158	3e−5	*Schizosaccharomyces pombe*, BAA06454 (SMC4, structural maintenance of chr4)	1e−80	*Canis familiaris*, XP_535848 (structural maintenance of chromosomes 4-like 1 protein)	1e−78

[a] NCBI database numbers.
[b] NCBI locus tag/accession number from the *E. histolytica* genome database at The Institute for Genomic Research.

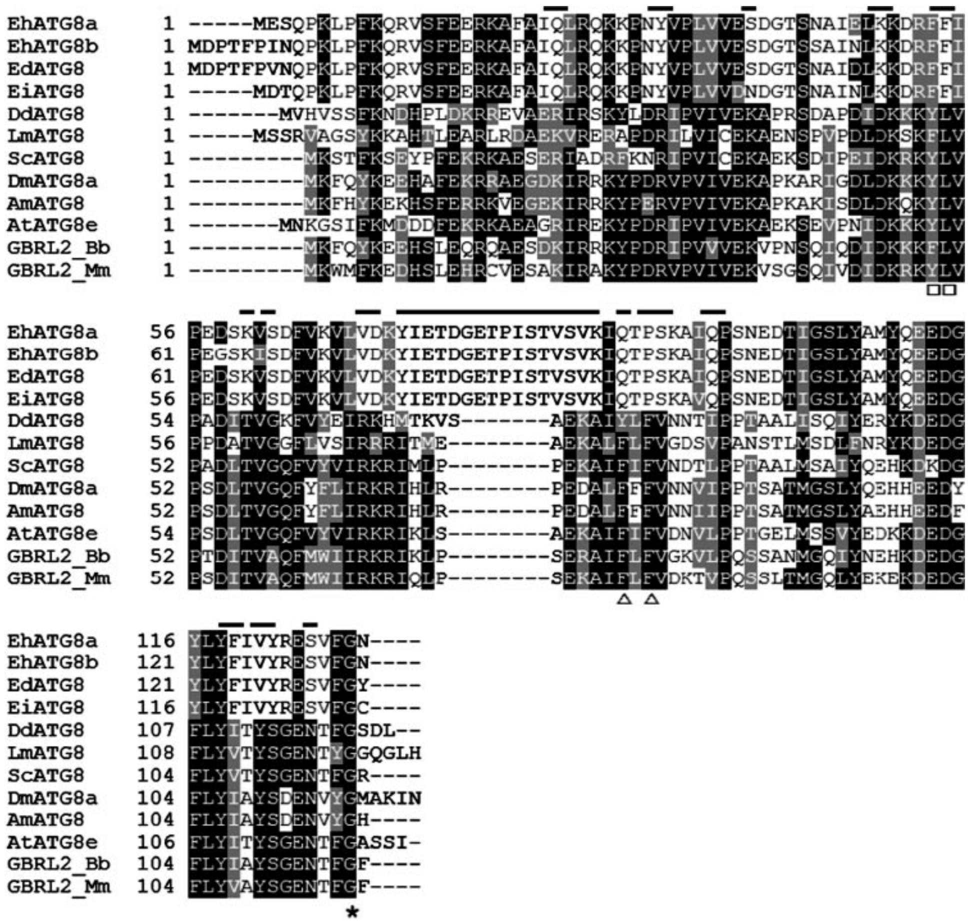

FIG. 1. Alignment of Atg8 protein sequences from three *Entamoeba* species and other organisms. Clustal W (http://www.ch.embnet.org/software/ClustalW.html) and BoxShade 3.21 (http://www.ch.embnet.org/software/BOX_form.html) were used to produce the alignment. Conserved amino acid residues are shown with a black background, and conserved substitutions are shown with a gray background. Gaps are shown by dashes. The asterisk under the alignment indicates the consensus glycine that is conjugated to PE. Residues implicated in binding to Atg4 and autophagy activity are depicted with triangles and squares under the alignment, respectively. *Entamoeba*-specific residues are overlined. Sequences used in the alignment were those for EdAtg8 (*E. dispar* genome accession no. AANV01003233), EiAtg8 (accession no. AANW01005912, nt 44 to 433), EhAtg8a (locus tag XP_649165), EhAtg8b (locus tag XP_649940), DdAtg8 (*Dictyostelium discoideum*, locus tag XP_637841), LmAtg8.1 (*Leishmania major*, EMBL accession no. CAJ07266), ScAtg8 (*Saccharomyces cerevisiae*, Swiss-Prot accession no. P38182), DmAtg8a (*Drosophila melanogaster*, locus tag NP_727447), AmAtg8 (*Apis mellifera*, locus tag XP_001120069), AtAtg8e (*Arabidopsis thaliana*, locus tag NP_182042), GBRL2_Bb (Gabarapl2 from *Branchiostoma belcheri*, accession no. AAO45172), and GBRL2_Mm (Gabarapl2 from *Mus musculus*, EMBL accession no. BAB22217).

shown). These EhAtg4s were previously reported as "autophagins 1 to 4," which are members of the C54 cysteine endopeptidase family (6). In yeast, only one isoform of Atg4 has been reported (53, 55), while *Homo sapiens* apparently possesses four Atg4 homologs (52). The putative Atg3 and Atg7 homologs (EhAtg3 and EhAtg7) showed 31 to 47% and 34 to 38% identities to yeast and mammalian counterparts, respectively. On the other hand, *E. histolytica* apparently lacks genes encoding Atg5, Atg10, Atg12, and Atg16 (Table 1).

The presence of the Atg8 conjugation system and the concomitant absence of the Atg5-to-Atg12 conjugation pathway were also reported for both the free-living social amoeba *Dictyostelium* (41) and the parasitic protist *Leishmania* (60). These data may indicate that the Atg8 conjugation system is evolutionarily older than the Atg5-to-Atg12 conjugation system and that the former represents minimal machinery required for autophagy. As shown below, the Atg8 conjugation system is apparently sufficient for autophagosome biogenesis, at least in these protists (4, 41).

Conservation of the Atg8 conjugation pathway in related *Entamoeba* species, namely, *E. dispar* and *E. invadens*. *E. dispar* is the commensal nonpathogenic species for mammals, while *E. invadens* is the invasive reptilian species and a primary model of encystation. Although the *E. dispar* and *E. invadens* genomes have not been completed, we identified two *Atg8* genes (locus tags AANV01003233 and AANV01014404), one *Atg4* gene (AANV01002875), two *Atg7* genes (AANV01000460 and AANV01009354), and one *Atg3* gene (AANV01000567) in the *E. dispar* database, while only one *Atg8* gene (AANW01005912, nucleotides [nt] 44 to 433), one *Atg4* gene (AANW01010411, nt 5 to 1166; the gene likely contains an intron, but the carboxyl terminus of the protein is incomplete), and one *Atg3* gene (AANW01009890, nt 424 to 1226 in a complementary strand) were found in the *E. invadens* genome database (data

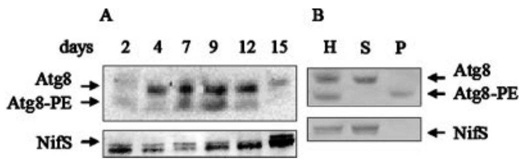

FIG. 2. Immunoblot analysis of Atg8 in *E. invadens*. (A) Immunoblot analysis of Atg8 in *E. invadens* trophozoites cultured in a normal proliferation medium. *E. invadens* trophozoites were cultivated in BI-S medium at the indicated times (days 2 to 15), and whole lysates were electrophoresed by SDS-PAGE, blotted, and reacted with anti-EhAtg8 (top panel) or a control antibody against EhNifS (1) (bottom panel). A representative blot from three independent experiments is shown. (B) Cell fractionation of Atg8. A whole lysate produced by mechanical homogenization of trophozoites, harvested 1 week after the initiation of the culture at a cell density of $\sim 5 \times 10^4$ cells/ml, was separated into the supernatant and pellet fractions by centrifugation at $100{,}000 \times g$ and subjected to immunoblot analysis as described above. Lane H, a whole homogenate; lane S or P, a supernatant or a pellet after centrifugation at $100{,}000 \times g$ centrifugation, respectively.

not shown). We were unable to identify an *Atg7* ortholog in the *E. invadens* genome, likely due to incomplete sequencing of the genome. Comparison of EiAtg8 and *E. dispar* Atg8 (EdAtg8) to EhAtg8a and EhAtg8b showed that EiAtg8 is 99% and 95% identical to EhAtg8a and EhAtg8b and that EdAtg8 is 98% and 96% identical to EhAtg8a and EhAtg8b, respectively. The high degree of conservation in *E. invadens* is remarkable considering that this species has shown itself to be largely divergent from *E. histolytica* and *E. dispar*, as indicated by the significant differences in codon usage and G-C content between *E. invadens* and *E. histolytica*/*E. dispar* (40).

Features of *Entamoeba* Atg8. Amino acid comparisons by using Clustal W (Fig. 1) highlighted a number of unique features of *Entamoeba* Atg8. Phe77 and Phe79 (numbered as for *Saccharomyces cerevisiae* Atg8), implicated in the interaction with Atg4 in yeast (2), are not conserved in Atg8 proteins from *Entamoeba* species but are well conserved in *Leishmania*, *Arabidopsis* spp., and mammals. Neither are other important

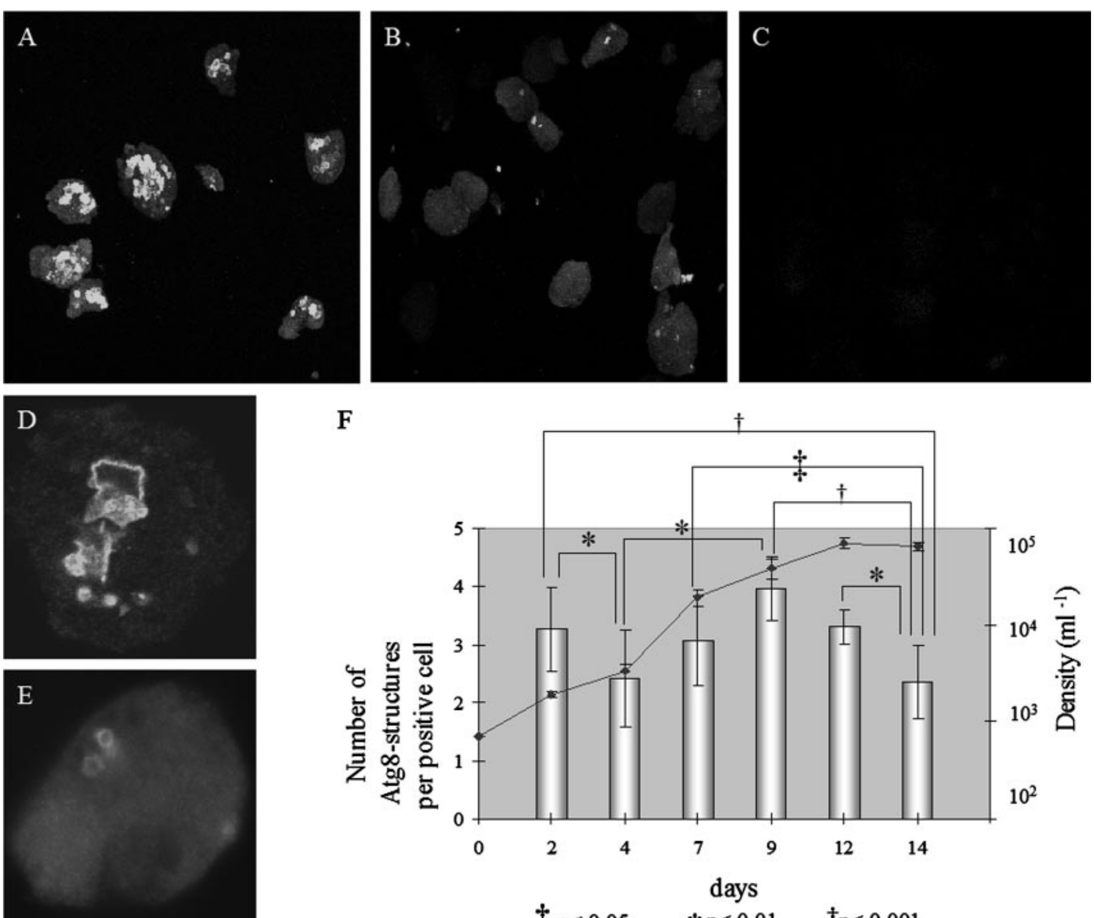

FIG. 3. Immunofluorescence imaging of autophagy in proliferating trophozoites of *E. invadens.* (A to C) Immunofluorescence images of Atg8 in proliferating *E. invadens*. Maximum-projection images of 8 to 10 *E. invadens* trophozoites of 1 (A)- and 2 (B)-week-old cultures reacted with anti-EhAtg8 antibody under low magnification are shown. One-week-old culture was also reacted with preimmune serum (C). (D to E) Confocal images under high magnification of a representative slice of a single typical trophozoite harvested at 1 week (D) or 2 weeks (E). (F) Growth kinetics of *E. invadens* trophozoites and autophagosome formation in the normal proliferation medium. Cell density was measured in triplicate, and the means and standard deviations are shown with diamonds connected by a solid line. Trophozoites in proliferation were assayed by immunofluorescence as previously described; the average numbers of Atg8-positive structures per positive cell were counted and are shown by the bars. Approximately 30 to 40 cells were examined at each time point. Pairwise comparisons between each time point, with statistical significance (P value of <0.001, <0.01, or <0.05), are also indicated.

residues involved in the autophagy activity in yeast (Tyr49 and Leu50) (2) conserved in *Entamoeba* Atg8. A number of other residues totally conserved in Atg8 proteins from other organisms are not conserved in *Entamoeba*; these residues are distributed throughout the entire protein (Fig. 1).

All *Entamoeba* Atg8s share a unique 16-amino acid insertion (e.g., amino acids 72 to 88 of EhAtg8a; YIETDGETPISTVS VK). Based on the crystal structure of Atg8 from yeast, this region is located 1 to 5 residues upstream of the Atg4 recognition site (Phe-X-Phe, which is absent in *Entamoeba* Atg8) and thus predicted to be exposed on the surface of the molecule and possibly interacts with other proteins. We also examined the nucleotide sequence of this region of all *Entamoeba Atg8* genes and excluded the possibility that this region corresponds to an intron by reverse transcriptase PCR of cDNA (data not shown). EhAtg8b has an extra 5-amino-acid amino-terminal extension (MDPTF), which is also present in EdAtg8 but missing in EiAtg8. Interestingly, the overall identities of EdAtg8 and EiAtg8 to EhAtg8a or EhAtg8b are not consistent with the fact that EiAtg8 lacks the 5-amino-acid amino-terminal extension present in EhAtg8b but that EdAtg8 possesses it. It is unlikely that the lack of this amino-terminal extension in EiAtg8 is due to an incomplete genome database because the open reading frame of Ei*Atg8* is not located at the end of the contig AANW01005912 (nt 44 to 433 of the total length of 1,166 nt).

Immunoblot analysis of Atg8 in *E. invadens*. In order to verify if autophagy occurs in *Entamoeba* and, if it does, to identify growth phases and stages where autophagy plays a role, immunoblot analysis of *E. invadens* trophozoites cultured in a regular proliferation medium with anti-EhAtg8 antibody was conducted (Fig. 2). Two bands with molecular masses of approximately 15.0 and 14.5 kDa were observed (Fig. 2A). Dramatic changes in both the total amount of Atg8 and the proportions of the two forms were found during 2 weeks of culture. The intensity of both the 15.0- and 14.5-kDa Atg8 bands increased in the mid- and late-logarithmic growth phases (days 4 to 12) and peaked at day 9, while it decreased at days 2 and 15. The ratios of the intensity of the 15.0-kDa band to that of the 14.5-kDa band were 2.4, 1.4, 1.1, and 2.2 at days 4, 7, 9, and 12, respectively, based on chemiluminescence measurements of these bands (data not shown). These data correlate well with the results of the immunofluorescence study (Fig. 3) (see below).

Cell fractionation followed by immunoblot assay (Fig. 2B) showed that 15.0-kDa Atg8 was fractionated almost exclusively to the soluble, likely cytosolic, fraction but that the 14.5-kDa Atg8 was found in the pellet fraction centrifuged at 100,000 $\times$ *g*. On the basis of the results of a number of other studies (17, 20), we concluded that the top band corresponds to the cytosolic, nonconjugated Atg8 protein and that the bottom band corresponds to the membrane-associated PE-conjugated Atg8 protein.

Immunofluorescence imaging of Atg8 in proliferating *E. invadens* trophozoites. Immunofluorescence analysis revealed remarkable changes in the Atg8-associated autophagosome-like structures in *E. invadens* trophozoites in both the logarithmic and stationary growth phases. Microscopic images of cultures at representative time points—1 and 2 weeks—under low magnification showed homogeneous Atg8 staining in each population, but remarkable differences in intensity were observed between 1- and 2-week-old cultures (Fig. 3A and B). In order to further investigate the observed growth-phase-dependent synthesis and degradation of autophagosomes, we quantified the number of Atg8-associated structures, examined under high magnification, during the exponential to stationary growth phases (Fig. 3D to F). The average number of Atg8-associated autophagosome-like structures (see below for morphological categories) peaked at 9 days in the BI-S-33 proliferation medium. Although the number of Atg8-associated structures was more than three per cell at day 2, the structures were mainly dot-like or tiny vesicles (data not shown), which is consistent with the repression of *Atg8* demonstrated by immunoblot analysis.

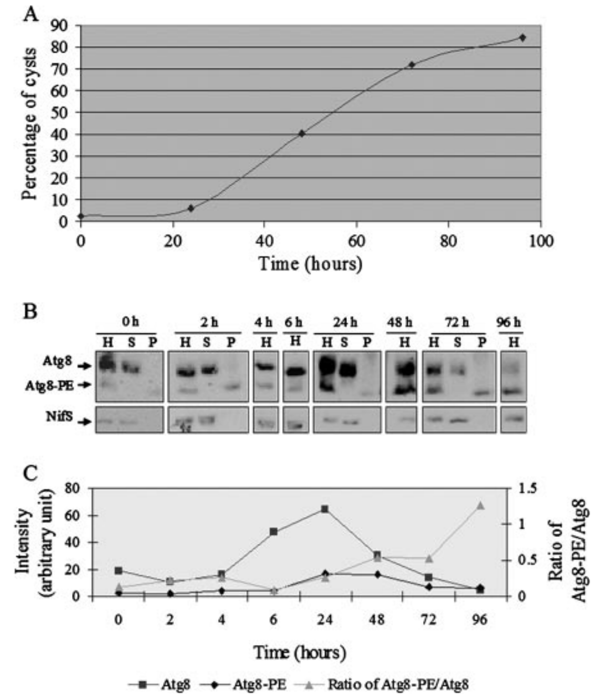

FIG. 4. Immunoblot analysis of Atg8 in *E. invadens* during encystation. (A) Kinetics of encystation. The percentages of the amoebae resistant to 0.05% Sarkosyl during encystation are shown. (B) *E. invadens* trophozoites were harvested at the indicated times, lysed, fractionated as described for Fig. 2B, and subjected to immunoblot analysis by using anti-EhAtg8 (top panel) or anti-EhNifS (bottom panel) antibody, followed by chemiluminescence detection. Lanes: H, whole homogenate; S and P, supernatant and pellet, respectively, after centrifugation at 100,000 $\times$ *g*. (C) Densitometric measurements from immunoblots developed by chemiluminescence. Only representative quantitations from three immunoblots which exhibited similar kinetics are shown.

Expression and membrane recruitment of Atg8 change during encystation in *E. invadens*. Autophagy has recently been implicated in differentiation during nutrient deprivation in organisms such as *C. elegans*, *D. discoideum*, and *Leishmania* (4, 34, 41, 60). Although it has recently been demonstrated that encystation-specific genes could be identified in *E. histolytica* clinical isolates (10), in vitro encystation of both *E. histolytica* clinical isolates and laboratory strains has not been accomplished. To further investigate if autophagy is induced during encystation, we exploited the encystation of *E. invadens* with

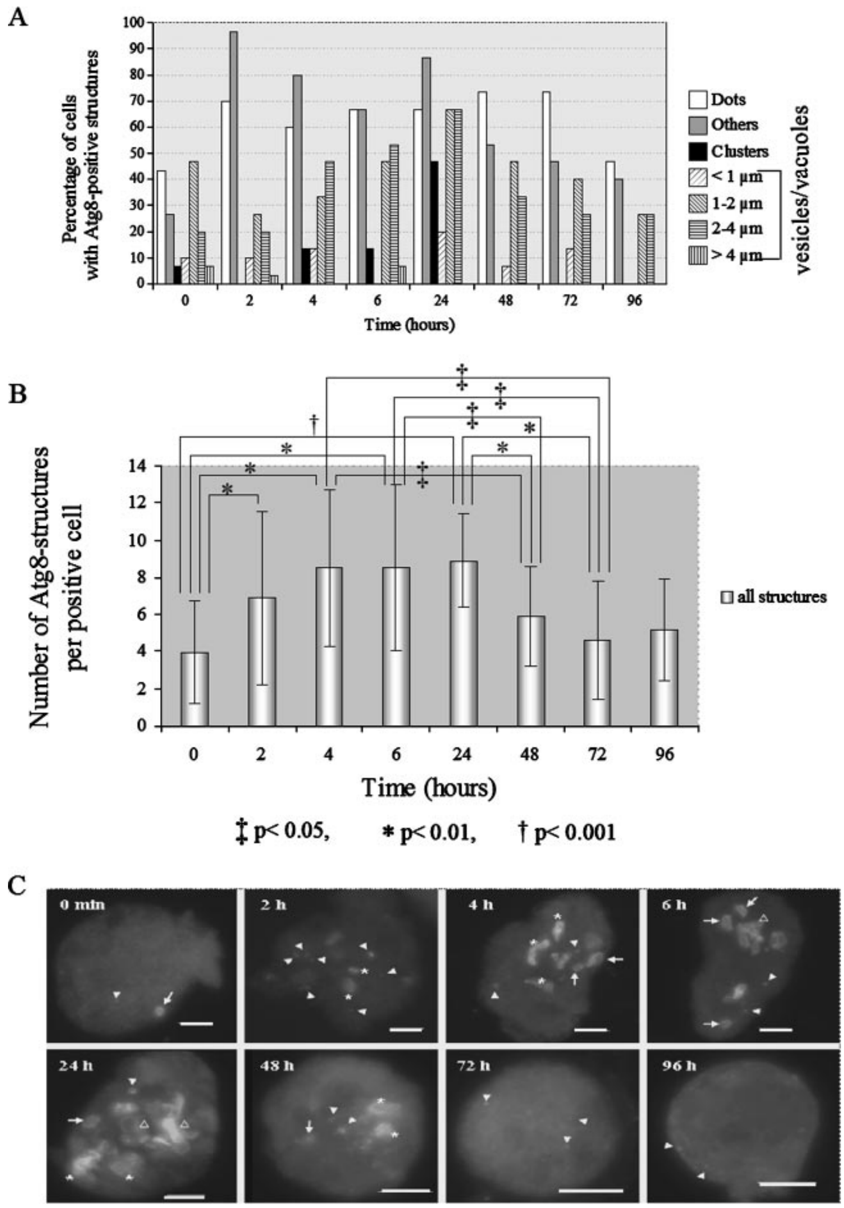

FIG. 5. Kinetics of Atg8-positive autophagosome-like structures during encystation by immunofluorescence assays. (A) Percentages of amoebae containing categorized Atg8-positive structures during encystation are shown. The categories are cytosolic; dot-like; vesicles/vacuoles with diameters of <1.0 μm, 1.0 to 2.0 μm, 2.0 to 4.0 μm, and >4.0 μm; other structures; and clusters. (B) Average numbers of Atg8 structures, as categorized above, per positive amoeba. Approximately 30 to 40 cells were examined at each time point, and means and standard deviations are shown. Pairwise comparisons between each time point, with statistical significance (*P* value of <0.001, <0.01, or <0.05), are also indicated. Representative results of three independent experiments are shown in panels A and B. (C) Subcellular localization of Atg8 during encystation. Representative images of a maximum projection of approximately 20 slices taken at 1-μm intervals on the *z* axis at each time point are shown. Filled arrowheads, open arrowheads, arrows, and asterisks indicate Atg8-positive dot-like structures, clusters, vesicles/vacuoles, and other structures, respectively. Bars = 5 μm.

2-week-old cultures as an inoculum into the 47% LG medium lacking glucose. Under these conditions, we accomplished up to 80 to 93% encystation within 96 h, based on Sarkosyl resistance (Fig. 4A). We also verified that the kinetics of the increment of Sarkosyl-resistant amoebae and that of the calcofluor-stained amoebae were almost indistinguishable (data not shown). Although encystation is usually induced in trophozoites using 2- to 3-day-old cultures (12) or 7-day-old cultures in the logarithmic growth phase (32), we used 2-week-old cultures as an inoculum. As described above, the amount of Atg8 protein and the number of membrane-associated Atg8-positive structures were significantly lower in the 2-week-old cultures than in the 2- to 7-day-old cultures, and thus the kinetics of Atg8 synthesis and the formation of the Atg8-positive structures during encystation could ideally be monitored by using 2-week-old cultures.

Amoebae were harvested at various time points, and Atg8 was first examined by immunoblotting and quantitated as de-

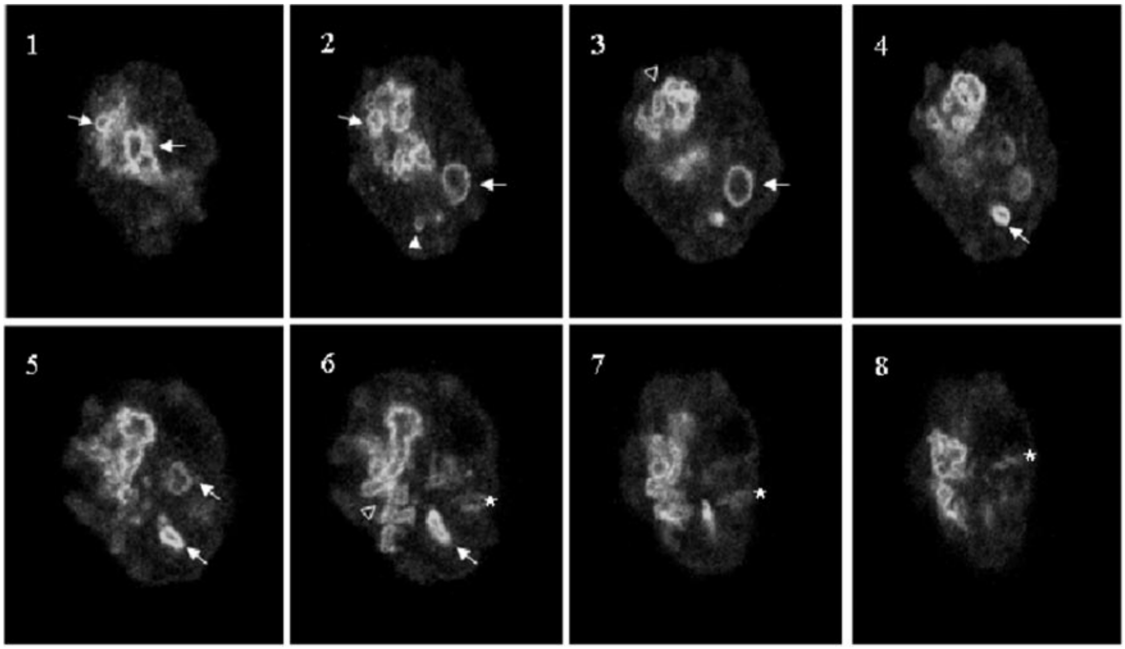

FIG. 6. Confocal images of Z stacks of an encysting *E. invadens* trophozoite. *E. invadens* trophozoites were incubated in 47% LG medium for 24 h and analyzed by immunofluorescence assay with anti-EhAtg8 antibody and Alexa 488-conjugated anti-rabbit IgG antibody. Eight slices of a representative trophozoite were captured at 1-μm intervals on the *z* axis and are shown from the bottom to the top. A filled arrowhead, an open arrowhead, arrows, and asterisks indicate representative Atg8-positive dot-like structures, clusters, vesicles/vacuoles, and other structures, respectively.

scribed above (Fig. 4B and C). The amount of unmodified Atg8 was reduced as early as 2 h after the amoebae were transferred to the encystation medium. Concomitantly, the amount of PE-modified Atg8 increased and peaked at 24 to 48 h. The total amount of Atg8, estimated by chemiluminescence assay, changed during encystation. The ratio of PE-conjugated Atg8 to unmodified Atg8 also changed significantly. The ratio of Atg8-PE to unmodified Atg8 also increased in a course of encystation (e.g., 0.09 or 1.26 at 6 or 96 h, respectively). These data are similar to the observation about the formation of autophagosomes under starvation conditions in other organisms (19). Interestingly, at 24 h after the induction of encystation, the production of PE-modified Atg8 reached a plateau, while only 7% of the trophozoites differentiated into cysts, as evaluated by detergent resistance (Fig. 4A) and calcofluor staining (data not shown). Thus, the emergence of PE-conjugated Atg8 precedes encystation. To verify that autophagy really occurs in encysting cells, we examined the presence of Atg8-associated structures in detergent-resistant cysts after Sarkosyl treatment. Although we were unable to simultaneously examine cyst markers and Atg8 due to technical problems (i.e., calcofluor cannot be used in an immunofluorescence assay), these data are consistent with the premise that cluster formation increases as encystation proceeds.

Immunofluorescence assay reveals dramatic changes in the autophagosome-like structures during encystation. Immunofluorescence imaging of encysting *E. invadens* cultivated in 47% LG medium showed that both the percentage of amoeba-containing structures and the number of structures per amoeba increased during encystation (Fig. 5). Representative stacks of Atg8 structures at 24 h after the induction of *E. invadens* encystation are shown in Fig. 6. We morphologically categorized the Atg8-associated structures into several groups: "dots" (containing no luminal region); "vesicles/vacuoles" of <1, 1 to 2, 2 to 4, or >4 μm in diameter (containing a luminal region surrounded by Atg8-positive structures); "others" (including linear or thread-like structures); and "clusters" (containing multiple dots, vesicles, vacuoles, and other structures) (Fig. 5A and C). Atg8-positive dots and other structures, including linear and diffuse/amorphous structures, were observed in almost all cells in the population. As early as 2 h after the induction of encystation, both the percentages of cells containing the Atg8-positive dot-like and other structures and the numbers of these structures per cell started to increase, peaked at 24 h, and then gradually decreased from 24 to 96 h. Both the numbers and sizes of the vesicular/vacuolar structures increased from 4 to 24 h; e.g., at 24 h, approximately 65% of the amoebae contained large Atg8-positive vesicles/vacuoles 2 to 4 μm in diameter. The Atg8-positive clusters emerged mainly after 24 h. Concomitant with the emergence of the cluster structures, the percentage of cysts started to increase, suggesting that cluster formation may coincide with the initiation of morphological and biochemical encystation.

The dot structures observed in this study were similar to those typically referred to as PAS (Fig. 5C), which correspond to a perivacuolar site containing lipids and early autophagy proteins such as Atg8/LC3 (27). PAS undergoes elongation and originate double membranes called isolation membranes (36, 58). It was reported that in yeast, the diameter of the autophagosomes ranges from 0.3 to 0.9 μm (58), while it usually ranges up to 1.5 μm in mammals (e.g., embryonic stem cells, embryonic fibroblasts, hepatocytes, and pancreatic acinar

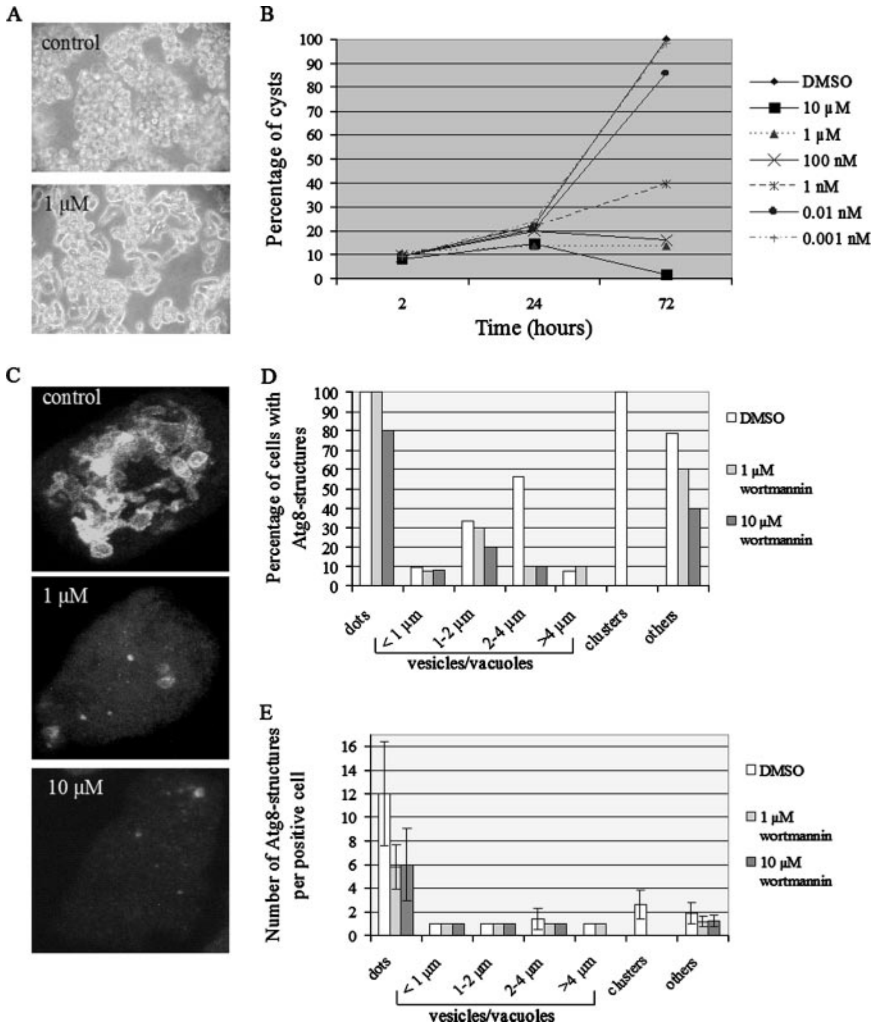

FIG. 7. Inhibition of encystation and the formation of autophagosomes by wortmannin in *E. invadens*. (A) Micrographs of amoebae at 72 h after induction of encystation with or without wortmannin. *E. invadens* trophozoites were incubated in 47% LG medium and supplemented with dimethyl sulfoxide (DMSO) (control) or 1 μM wortmannin. (B) Percentages of cysts after 2, 24, or 72 h of incubation in the encystation medium with various concentrations of wortmannin. The results of a representative set of three independent experiments are shown. (C) Immunofluorescence images of EiAtg8-positive structures in cells not treated or treated with 1 or 10 μM wortmannin in the encystation medium for 2 days. Representative images of the maximum projection of approximately 20 slices taken at 1-μm intervals on the *z* axis are shown. (D) Percentages of amoebae containing categorized Atg8-positive structures during encystation in the presence of 1 or 10 μm wortmannin are shown. (E) Average numbers of Atg8-positive structures per positive amoeba in the absence or presence of 1 or 10 μM wortmannin. Representative results of three independent experiments are shown.

cells) (35). Therefore, the sizes of the Atg8-associated autophagosome-like structures in *Entamoeba* shown in the present study are unprecedented, except for the 5- to 10-μm autophagosomes containing group A streptococci, *Mycobacterium tuberculosis*, and *Toxoplasma* (3, 13, 37). Under nonstarvation conditions, we found predominantly 1- to 2-μm Atg8-positive vesicles/vacuoles in proliferating trophozoites, suggesting that vesicles/vacuoles of this size represent autophagosomes constitutively formed under normal conditions. This is similar to what was reported for mammalian cells where autophagy was constitutively active or suppressed in response to specific hormones (58).

PI 3-kinase inhibitors abolish proliferation, encystation, and the formation of autophagosomes in *E. invadens*. The proliferation of trophozoites was severely affected by wortmannin, a well-known fungal phosphatidylinositol (PI) 3-kinase inhibitor, which was shown to inhibit autophagy in yeast, mammals, and *Leishmania* (4, 27). The growth of trophozoites cultivated in the BI-S-33 medium containing 1 μM wortmannin for 1 week was impaired by >90% (data not shown). Immunofluorescence analysis showed that the average number of the Atg8-associated structures decreased by 25% in trophozoites treated with the inhibitor (data not shown).

We next examined the effects of the inhibition of PI 3-kinase by wortmannin or 3-methyladenine during encystation. Wortmannin at ≥100 nM completely inhibited encystation as measured by Sarkosyl resistance at 72 h (Fig. 7B). Concomitantly, 1 μM of wortmannin also inhibited the rounding and agglutination of parasites, which was normally observed during encystation (Fig. 7A). These data are consistent with previous findings (31). The immunofluorescence assay showed that the formation of Atg8-associated structures was abolished by wortmannin (Fig. 7C to E). Both the percentage of positive cells and the number of Atg8-associated clusters and vesicles/vacuoles, particularly those 2 to 4 μm and >4 μm in diameter, per cell significantly decreased after wortmannin treatment (Fig. 7D and E). Although the percentage of cells containing dots did not change, the average number of these punctate structures, which presumably correspond to PAS, was reduced by 50% ($P < 0.05$). The simultaneous dose-dependent inhibition of encystation and the autophagosome formation are consistent with the involvement of PI 3-kinase in the biogenesis, most likely by fusion and/or aggregation, of autophagosomes in *Entamoeba* and with the fact that autophagy plays an important role in encystation. Both encystation and the formation of Atg8-associated structures were also simultaneously inhibited by 3-methyladenine, although the effective concentrations were >100-fold higher than those of wortmannin (data not shown). It was previously shown that wortmannin inhibits PI 3-kinases with a 50% inhibitory concentration of ~10 nM and that 3-methyladenine is less potent than wortmannin (its 50% inhibitory concentration is $\sim 10^6$-fold higher than that of wortmannin) (27). Wortmannin and 3-methyladenine inhibit the class III PI 3-kinases, including Vps34 (42), which forms PI 3-kinase complex I (58), an essential component of PAS (36), by competition with ATP binding (27). *E. histolytica* apparently possesses at least three—*Vps34* (locus tag XP_656932), *Vps15* (XP_652375), and *Apg6/Beciclin 1* (XP_656050)—of the four components necessary to form the PI 3-kinase complex, while the remaining component, *Apg14*, is absent from its genome. However, since proliferation, autophagy, and survival were shown to be regulated by Tor kinase, a class I and III PI 3-kinase (25, 27, 48, 56), the possibility that the defect of proliferation or encystation is not causally connected but simply coincides with the inhibition of autophagy cannot be excluded.

Significance of autophagy in *Entamoeba*. The presence of autophagosome-like structures in proliferating trophozoites of both *E. invadens* and *E. histolytica* (data not shown but described elsewhere) suggests a housekeeping role for autophagy in this group of protists. The remarkable increase in the formation of autophagosomes in the mid- to late logarithmic growth phase and their repression in the stationary phase are consistent with the hypothesis that autophagy likely plays a role in proliferation but not in survival during starvation. The involvement of autophagy during proliferation was also suggested for mouse T cells (43).

In addition to the role of autophagosomes in proliferation, their dramatic formation during the encystation of *E. invadens* strongly suggests that autophagy is involved in differentiation. The fact that the emergence of the Atg8-associated structures precedes morphological and biochemical changes (7, 10, 12, 47) during encystation strongly indicates that autophagy is a prerequisite for and plays an important role in encystation. It is also important to note that most of the differentially expressed genes previously identified (47) were up-regulated between 22 and 24 h after encystation induction, which coincides with the peak of autophagosome formation. The rapid degradation and recycling of cellular components via autophagy may be advantageous during encystation, which requires the dramatic and swift reorganization of cellular structures and organelles.

ACKNOWLEDGMENTS

We thank Asao Makioka, Jikei University, for providing the IP-1 strain and also technical help; Dan Sato for purification of the anti-EhAtg8 antibody; Yoko Yamada for production of the antibody; Eiryo Kawakami, University of Tokyo, for technical help; and all members of our laboratory for their technical assistance and discussions.

This work was supported in part by Grants-in-Aid for Scientific Research from the Ministry of Education, Culture, Sports, Science and Technology of Japan (17390124, 17790282, 18050006, 18073001); a grant for Research on Emerging and Reemerging Infectious Diseases from the Ministry of Health, Labor and Welfare (01712004); and a grant for the Project to Promote the Development of Anti-AIDS Pharmaceuticals from the Japan Health Sciences Foundation (KA11501) to T.N.

REFERENCES

1. **Ali, V., Y. Shigeta, U. Tokumoto, Y. Takahashi, and T. Nozaki.** 2004. An intestinal parasitic protist, Entamoeba histolytica, possesses a non-redundant nitrogen fixation-like system for iron-sulfur cluster assembly under anaerobic conditions. J. Biol. Chem. **279:**16863–16874.
2. **Amar, N., G. Lustig, Y. Ichimura, Y. Ohsumi, and Z. Elazar.** 2006. Two newly identified sites in the ubiquitin-like protein Atg8 are essential for autophagy. EMBO Rep. **7:**635–642.
3. **Andrade, R. M., M. Wessendarp, M. J. Gubbels, B. Striepen, and C. S. Subauste.** 2006. CD40 induces macrophage anti-*Toxoplasma gondii* activity by triggering autophagy-dependent fusion of pathogen-containing vacuoles and lysosomes. J. Clin. Investig. **116:**2366–2377.
4. **Besteiro, S., R. A. Williams, L. S. Morrison, G. H. Coombs, and J. C. Mottram.** 2006. Endosome sorting and autophagy are essential for differentiation and virulence of *Leishmania major*. J. Biol. Chem. **281:**11384–11396.
5. **Campos-Gongora, E., F. Ebert, U. Willhoeft, S. Said-Fernandez, and E. Tannich.** 2004. Characterization of chitin synthases from *Entamoeba*. Protist **155:**323–330.
6. **Clark, C. G., C. M. Alsmark, M. Hofer, Y. Saito-Nakano, V. Ali, S. Marion, C. Weber, C. Mukherjee, I. Bruchhaus, E. Tannich, M. Leippe, T. Sicheritz-Ponten, P. G. Foster, J. Samuelson, C. J. Noel, R. P. Hirt, T. M. Embley, C. A. Gilchrist, B. J. Mann, U. Singh, J. P. Acmers, S. Bhattacharya, A. Bhattacharya, A. Lohia, N. Guillen, M. Duchene, T. Nozaki, and N. Hall.** Structure and content of *Entamoeba histolytica* genome. Adv. Parasitol., in press.
7. **Coppi, A., and D. Eichinger.** 1999. Regulation of *Entamoeba invadens* encystation and gene expression with galactose and N-acetylglucosamine. Mol. Biochem. Parasitol. **102:**67–77.
8. **Diamond, L. S., C. F. T. Mattern, and I. L. Bartgis.** 1972. Viruses of *Entamoeba histolytica*. J. Virol. **9:**326–341.
9. **Doelling, J. H., J. M. Walker, E. M. Friedman, A. R. Thompson, and R. D. Vierstra.** 2002. The APG8/12-activating enzyme APG7 is required for proper nutrient recycling and senescence in *Arabidopsis thaliana*. J. Biol. Chem. **277:**33105–33114.
10. **Ehrenkaufer, G. M., R. Haque, J. A. Hackney, D. J. Eichinger, and U. Singh.** 2007. Identification of developmentally regulated genes in *Entamoeba histolytica*: insights into mechanisms of stage conversion in a protozoan parasite. Cell. Microbiol. **9:**1426–1444.
11. **Eichinger, D.** 2001. Encystation in parasitic protozoa. Curr. Opin. Microbiol. **4:**421–426.
12. **Gonzalez, J., G. Bai, U. Frevert, E. J. Corey, and D. Eichinger.** 1999. Proteasome-dependent cyst formation and stage-specific ubiquitin mRNA accumulation in *Entamoeba invadens*. Eur. J. Biochem. **264:**897–904.
13. **Gutierrez, M. G., S. S. Master, S. B. Singh, G. A. Taylor, M. I. Colombo, and V. Deretic.** 2004. Autophagy is a defense mechanism inhibiting BCG and *Mycobacterium tuberculosis* survival in infected macrophages. Cell **119:**753–766.
14. **Hamasaki, M., T. Noda, and Y. Ohsumi.** 2003. The early secretory pathway contributes to autophagy in yeast. Cell Struct. Funct. **28:**49–54.
15. **Huang, W. P., and D. J. Klionsky.** 2002. Autophagy in yeast: a review of the molecular machinery. Cell Struct. Funct. **27:**409–420.
16. **Ichimura, Y., Y. Imamura, K. Emoto, M. Umeda, T. Noda, and Y. Ohsumi.** 2004. In vivo and in vitro reconstitution of Atg8 conjugation essential for autophagy. J. Biol. Chem. **279:**40584–40592.
17. **Ichimura, Y., T. Kirisako, T. Takao, Y. Satomi, Y. Shimonishi, N. Ishihara, N. Mizushima, I. Tanida, E. Kominami, M. Ohsumi, T. Noda, and Y. Ohsumi.** 2000. A ubiquitin-like system mediates protein lipidation. Nature **408:**488–492.
18. **Ishihara, N., M. Hamasaki, S. Yokota, K. Suzuki, Y. Kamada, A. Kihara, T. Yoshimori, T. Noda, and Y. Ohsumi.** 2001. Autophagosome requires specific

early Sec proteins for its formation and NSF/SNARE for vacuolar fusion. Mol. Biol. Cell **12:**3690–3702.
19. **Kabeya, Y., N. Mizushima, T. Ueno, A. Yamamoto, T. Kirisako, T. Noda, E. Kominami, Y. Ohsumi, and T. Yoshimori.** 2000. LC3, a mammalian homologue of yeast Apg8p, is localized in autophagosome membranes after processing. EMBO J. **19:**5720–5728.
20. **Kirisako, T., Y. Ichimura, H. Okada, Y. Kabeya, N. Mizushima, T. Yoshimori, M. Ohsumi, T. Takao, T. Noda, and Y. Ohsumi.** 2000. The reversible modification regulates the membrane-binding state of Apg8/Aut7 essential for autophagy and the cytoplasm to vacuole targeting pathway. J. Cell Biol. **151:**263–276.
21. **Klionsky, D. J., J. M. Cregg, W. A. Dunn, Jr., S. D. Emr, Y. Sakai, I. V. Sandoval, A. Sibirny, S. Subramani, M. Thumm, M. Veenhuis, and Y. Ohsumi.** 2003. A unified nomenclature for yeast autophagy-related genes. Dev. Cell **5:**539–545.
22. **Kuma, A., N. Mizushima, N. Ishihara, and Y. Ohsumi.** 2002. Formation of the approximately 350-kDa Apg12-Apg5.Apg16 multimeric complex, mediated by Apg16 oligomerization, is essential for autophagy in yeast. J. Biol. Chem. **277:**18619–18625.
23. **Levine, B.** 2005. Eating oneself and uninvited guests: autophagy-related pathways in cellular defense. Cell **120:**159–162.
24. **Levine, B., and D. J. Klionsky.** 2004. Development by self-digestion: molecular mechanisms and biological functions of autophagy. Dev. Cell **6:**463–477.
25. **Levine, B., and J. Yuan.** 2005. Autophagy in cell death: an innocent convict? J. Clin. Investig. **115:**2679–2688.
26. **Liang, K., Y. Lin, Y. Zhang, Z. Chen, P. Zhang, and H. Zhang.** 2004. Developmental expression of amphioxus GABAA receptor-associated protein-like 2 gene. Dev. Genes Evol. **214:**339–341.
27. **Lindmo, K., and H. Stenmark.** 2006. Regulation of membrane traffic by phosphoinositide 3-kinases. J. Cell Sci. **119:**605–614.
28. **Ling, Y. M., M. H. Shaw, C. Ayala, I. Coppens, G. A. Taylor, D. J. Ferguson, and G. S. Yap.** 2006. Vacuolar and plasma membrane stripping and autophagic elimination of *Toxoplasma gondii* in primed effector macrophages. J. Exp. Med. **203:**2063–2071.
29. **Liu, Y., M. Schiff, K. Czymmek, Z. Talloczy, B. Levine, and S. P. Dinesh-Kumar.** 2005. Autophagy regulates programmed cell death during the plant innate immune response. Cell **121:**567–577.
30. **Lum, J. J., R. J. DeBerardinis, and C. B. Thompson.** 2005. Autophagy in metazoans: cell survival in the land of plenty. Nat. Rev. Mol. Cell Biol. **6:**439–448.
31. **Makioka, A., M. Kumagai, H. Ohtomo, S. Kobayashi, and T. Takeuchi.** 2001. Inhibition of encystation of *Entamoeba invadens* by wortmannin. Parasitol. Res. **87:**371–375.
32. **Makioka, A., M. Kumagai, H. Ohtomo, S. Kobayashi, and T. Takeuchi.** 2000. Effect of the antitubulin drug oryzalin in the encystation of *Entamoeba invadens*. Parasitol. Res. **86:**625–629.
33. **Martinez-Palomo, A., and M. Martinez-Baez.** 1983. Selective primary health care: strategies for control of disease in the developing world. X. Amebiasis. Rev. Infect. Dis. **5:**1093–1102.
34. **Melendez, A., Z. Talloczy, M. Seaman, E. L. Eskelinen, D. H. Hall, and B. Levine.** 2003. Autophagy genes are essential for dauer development and life-span extension in *C. elegans*. Science **301:**1387–1391.
35. **Mizushima, N., Y. Ohsumi, and T. Yoshimori.** 2002. Autophagosome formation in mammalian cells. Cell Struct. Funct. **27:**421–429.
36. **Nair, U., and D. J. Klionsky.** 2005. Molecular mechanisms and regulation of specific and nonspecific autophagy pathways in yeast. J. Biol. Chem. **280:**41785–41788.
37. **Nakagawa, I., A. Amano, N. Mizushima, A. Yamamoto, H. Yamaguchi, T. Kamimoto, A. Nara, J. Funao, M. Nakata, K. Tsuda, S. Hamada, and T. Yoshimori.** 2004. Autophagy defends cells against invading group A *Streptococcus*. Science **306:**1037–1040.
38. **Nimmerjahn, F., S. Milosevic, U. Behrends, E. M. Jaffee, D. M. Pardoll, G. W. Bornkamm, and J. Mautner.** 2003. Major histocompatibility complex class II-restricted presentation of a cytosolic antigen by autophagy. Eur. J. Immunol. **33:**1250–1259.
39. **Nozaki, T., T. Asai, S. Kobayashi, F. Ikegami, M. Noji, K. Saito, and T. Takeuchi.** 1998. Molecular cloning and characterization of the genes encoding two isoforms of cysteine synthase in the enteric protozoan parasite *Entamoeba histolytica*. Mol. Biochem. Parasitol. **97:**33–44.
40. **Nozaki, T., T. Asai, and T. Takeuchi.** 1997. Codon usage in *Entamoeba histolytica*, *E. dispar* and *E. invadens*. Parasitol. Int. **46:**105–109.
41. **Otto, G. P., M. Y. Wu, N. Kazgan, O. R. Anderson, and R. H. Kessin.** 2003. Macroautophagy is required for multicellular development of the social amoeba *Dictyostelium discoideum*. J. Biol. Chem. **278:**17636–17645.
42. **Petiot, A., E. Ogier-Denis, E. F. Blommaart, A. J. Meijer, and P. Codogno.** 2000. Distinct classes of phosphatidylinositol 3′-kinases are involved in signaling pathways that control macroautophagy in HT-29 cells. J. Biol. Chem. **275:**992–998.
43. **Pua, H. H., I. Dzhagalov, M. Chuck, N. Mizushima, and Y. W. He.** 2007. A critical role for the autophagy gene Atg5 in T cell survival and proliferation. J. Exp. Med. **204:**25–31.
44. **Qu, X., J. Yu, G. Bhagat, N. Furuya, H. Hibshoosh, A. Troxel, J. Rosen, E. L. Eskelinen, N. Mizushima, Y. Ohsumi, G. Cattoretti, and B. Levine.** 2003. Promotion of tumorigenesis by heterozygous disruption of the beclin 1 autophagy gene. J. Clin. Investig. **112:**1809–1820.
45. **Reggiori, F., T. Shintani, U. Nair, and D. J. Klionsky.** 2005. Atg9 cycles between mitochondria and the pre-autophagosomal structure in yeasts. Autophagy **1:**101–109.
46. **Sambrook, J., and D. W. Russell.** 2001. Molecular cloning: a laboratory manual, 3rd ed. Cold Spring Harbor Laboratory Press, Cold Spring Harbor, NY.
47. **Sanchez, L., V. Enea, and D. Eichinger.** 1994. Identification of a developmentally regulated transcript expressed during encystation of Entamoeba invadens. Mol. Biochem. Parasitol. **67:**125–135.
48. **Sarbassov, D. D., S. M. Ali, and D. M. Sabatini.** 2005. Growing roles for the mTOR pathway. Curr. Opin. Cell Biol. **17:**596–603.
49. **Schmid, D., J. Dengjel, O. Schoor, S. Stevanovic, and C. Munz.** 2006. Autophagy in innate and adaptive immunity against intracellular pathogens. J. Mol. Med. **84:**194–202.
50. **Shintani, T., W. P. Huang, P. E. Stromhaug, and D. J. Klionsky.** 2002. Mechanism of cargo selection in the cytoplasm to vacuole targeting pathway. Dev. Cell **3:**825–837.
51. **Strawbridge, A. B., and J. S. Blum.** 2007. Autophagy in MHC class II antigen processing. Curr. Opin. Immunol. **19:**87–92.
52. **Sugawara, K., N. N. Suzuki, Y. Fujioka, N. Mizushima, Y. Ohsumi, and F. Inagaki.** 2005. Structural basis for the specificity and catalysis of human Atg4B responsible for mammalian autophagy. J. Biol. Chem. **280:**40058–40065.
53. **Suzuki, K., Y. Kubota, T. Sekito, and Y. Ohsumi.** 2007. Hierarchy of Atg proteins in pre-autophagosomal structure organization. Genes Cells **12:**209–218.
54. **Tanida, I., T. Ueno, and E. Kominami.** 2004. LC3 conjugation system in mammalian autophagy. Int. J. Biochem. Cell Biol. **36:**2503–2518.
55. **Tsukada, M., and Y. Ohsumi.** 1993. Isolation and characterization of autophagy-defective mutants of *Saccharomyces cerevisiae*. FEBS Lett. **333:**169–174.
56. **Uritani, M., H. Hidaka, Y. Hotta, M. Ueno, T. Ushimaru, and T. Toda.** 2006. Fission yeast Tor2 links nitrogen signals to cell proliferation and acts downstream of the Rheb GTPase. Genes Cells **11:**1367–1379.
57. **Van Dellen, K. L., A. Chatterjee, D. M. Ratner, P. E. Magnelli, J. F. Cipollo, M. Steffen, P. W. Robbins, and J. Samuelson.** 2006. Unique posttranslational modifications of chitin-binding lectins of *Entamoeba invadens* cyst walls. Eukaryot. Cell **5:**836–848.
58. **Wang, C. W., and D. J. Klionsky.** 2003. The molecular mechanism of autophagy. Mol. Med. **9:**65–76.
59. Reference deleted.
60. **Williams, R. A., L. Tetley, J. C. Mottram, and G. H. Coombs.** 2006. Cysteine peptidases CPA and CPB are vital for autophagy and differentiation in *Leishmania mexicana*. Mol. Microbiol. **61:**655–674.
61. **World Health Organization/Pan American Health Organization.** 1997. Amoebiasis. Wkly. Epidemiol. Rec. **72:**97–99.
62. **Yoshimoto, K., H. Hanaoka, S. Sato, T. Kato, S. Tabata, T. Noda, and Y. Ohsumi.** 2004. Processing of ATG8s, ubiquitin-like proteins, and their deconjugation by ATG4s are essential for plant autophagy. Plant Cell **16:**2967–2983.
63. **Yue, Z., S. Jin, C. Yang, A. J. Levine, and N. Heintz.** 2003. Beclin 1, an autophagy gene essential for early embryonic development, is a haploinsufficient tumor suppressor. Proc. Natl. Acad. Sci. USA **100:**15077–15082.

Editor: W. A. Petri, Jr.